

Article

# Application of Carbon Dioxide Snow in Machining of CGI Using an Additively Manufactured Turning Tool

Thomas Heep \*, Christian Bickert and Eberhard Abele

Institute of Production Management, Technology and Machine Tools (PTW), Technical University of Darmstadt, 64287 Darmstadt, Germany; cbickert@gmx.de (C.B.); e.abele@ptw.tu-darmstadt.de (E.A.)

\* Correspondence: t.heep@ptw.tu-darmstadt.de; Tel.: +49-(0)6151-16-20119

Received: 24 December 2018; Accepted: 21 January 2019; Published: 23 January 2019



**Abstract:** The application of conventional cooling lubricants for the tribological conditioning of machining processes involves high additional costs and health risks. The application of a cryogenic carbon dioxide (CO<sub>2</sub>) snow cooling strategy is an economical and environmentally sound alternative for oily cooling emulsions since it has a high cooling effect as well as a residue-free sublimation. This article introduces a laser additive manufactured tool holder with an integrated dual nozzle which enables CO<sub>2</sub>-snow jet application. Initially this work focuses on the characterization and the selection of a suitable nozzle geometry. The modular tool body features an adapted channel structure for process-reliable and targeted CO<sub>2</sub>-snow cooling for turning processes. This enables the simultaneous cooling of the rake and flank face with CO<sub>2</sub>-snow, as well as the application of cryogenic multi-component cooling of the rake face. In the context of this study, the focus lies on the technological evaluation of three different supply strategies during the continuous turning of compacted graphite iron CGI-450 at increased cutting speed. It was established that an efficient rake face cooling is indispensable to achieve a low thermal tool load, and thus lower crater wear behavior. Therefore, this study contributes to an improvement in cryogenic machining processes regarding the design of additively manufactured tool bodies for process-reliable CO<sub>2</sub>-snow cooling, as well as for the selection of supply strategies to minimize the thermomechanical tool load.

**Keywords:** additively manufactured tools; carbon dioxide cooling; CGI machining

## 1. Introduction

Carbon dioxide (CO<sub>2</sub>), in the form of CO<sub>2</sub>-snow, and liquid nitrogen (LN<sub>2</sub>) are preferably used for the cryogenic cooling of machining applications [1]. Compared to LN<sub>2</sub>, the use of liquid CO<sub>2</sub> for cooling machining processes is easier to handle and more cost-effective. The application of CO<sub>2</sub> considerably minimizes cutting temperatures, which significantly increases tool operating times while simultaneously increasing productivity [2,3]. In previous work, the nozzle alignment for various cooling lubrication strategies (LN<sub>2</sub>, CO<sub>2</sub>-snow, minimum quantity lubrication, high-pressure cooling lubrication) in particular, could be identified as a significant influence parameter for the wear behavior of cutting materials [4–7].

Abele and Schramm [8] examined the performance of poly-crystalline diamond (PCD) and carbide cutting tools during the turning of vermicular cast iron while CO<sub>2</sub>-snow jets were applied to the rake face side. It is recommended to use cooled compressed air as well as CO<sub>2</sub>-snow to suppress thermally induced wear mechanisms when machining with PCD cutting materials with cutting speeds exceeding  $v_c = 190$  m/min. According to Pfeiffer [2], liquid CO<sub>2</sub> mass flux should be between 4.5 kg/h and 24 kg/h and CO<sub>2</sub> consumption should be adjusted depending on the present operating conditions. Furthermore, it was detected that the tool life decreases significantly with higher cutting speeds, due to the thermally induced wear process. The application of CO<sub>2</sub>-snow reduces the cutting temperature

significantly and enables a simultaneous increase in productivity and tool life. Up to now there are relatively few studies concerning the cooling with CO<sub>2</sub>-snow [9], even though handling liquid CO<sub>2</sub> is much simpler than liquid nitrogen [10–12].

To ensure a process-reliable and targeted cryogenic cooling process, a specially adapted feed system is required [13]. For example, continuous channel structures are necessary to prevent early expansion due to channel widening provoked by the physical properties of liquid CO<sub>2</sub>. Furthermore, the chosen nozzle concept is critical for attaining process reliability as well as the open jet properties. Lin et al. [14] examined the performance of CO<sub>2</sub>-snow nozzles in the area of medical endoscope technology and noted that the exclusive use of CO<sub>2</sub>-snow is problematic since there is a possibility of ice formation at the nozzle chamber or of the nozzle outlet. Therefore, the exclusive use of CO<sub>2</sub> is not suitable for long-term operations. A process-reliable operating behavior over a longer period of time can only be realized by applying an additional substance flow, consisting of e.g. dry air or nitrogen gas. Current studies in the area of machining of difficult-to-cut alloys, focus on the design of externally applied nozzle concepts for the supply of CO<sub>2</sub> in combination with MQL. For this purpose, Pereira et al. [15] carried out CFD simulations to examine the open jet behavior of CO<sub>2</sub> single component nozzles depending on the nozzle geometry. The use of a convergent shaped nozzle and a nozzle diameter of 1.5 mm gave promising results concerning the jet focus and the jet velocity.

Additively manufactured nozzle systems out of metal or plastic are already used for grinding applications [16]. Flow-optimized nozzle geometries can only be manufactured additively [17]. Powder-bed based procedures are suitable for processing metallic materials to produce high-quality components [18]. Thus, many additively manufactured tool structures reach the highest Technology Readiness Level, TRL 9 [19]. In the area of industrial machining, MAPAL [20] and KENNAMETAL [21] have patented the additive manufacturing of drilling tools equipped with cutting inserts. These tools are characterized by a defined porosity, grid-pattern structures and helical as well as variable channel cross-sections to ensure that the fed cooling lubricants can reach the highly-stressed tool areas. Furthermore, additively manufactured tool base bodies have spline shaped cooling channels [22] or carrier tools with a defined cavity design, known to reduce weight [23] and to passively absorb vibrations [24]. In a scientific environment, there are promising solutions for topologically optimized outer reamers [25] and turning tools [26], for internally cooled drilling tools [27] and turning tools [28] as well as for turning tools that enable targeted application of cryogenic CO<sub>2</sub>-snow jets [29,30].

On the one hand, the presented preliminary work shows the application potential of cryogenic CO<sub>2</sub>-snow to substitute potentially hazardous cooling emulsions and on the other hand, it shows the possibility of using a targeted application of CO<sub>2</sub>-snow as an option for machine resource-efficiency. Furthermore, there are various innovative design possibilities for the additive manufacturing of tool base bodies, which will increase the level of compactness as well as the functional integration in the future. However, there is still developmental scope regarding the compact implementation of cryogenic CO<sub>2</sub>-snow jets.

Thus, this work presents new design possibilities using a selective laser melting process to integrate a dual nozzle geometry into a modular tool holder to exploit the potential of cryogenic cooling and to apply it in a targeted and process-reliable way. To derive recommendations on the use and design, the cooling effect is examined with regard to the nozzle alignment as well as the nozzle load with a simplified method to measure heat transfer. Furthermore, shadow imaging is used to characterize the open jet properties when varying the nozzle outlet geometries. Subsequently, an additively manufactured turning tool holder with increased functionality and modular design is presented in this work, which, in addition to the simultaneous process cooling with CO<sub>2</sub>-snow on the rake face as well as on the flank face, enables the application of cryogenic multi-component cooling on the rake face.

## 2. Materials and Methods

A turning tool with an integrated dual nozzle was produced on a DMLS-system EOSINT M270 (EOS GmbH) at the Institute of Production Management, Technology and Machine Tools (PTW). For the construction material, a corrosion resistant steel “EOS Stainless Steel GP1”, which corresponds to the European material number 1.4542 was used.

The influence of nozzle alignment and nozzle load on the cooling effect was examined using the determined cooling rate with the differentiation and the absolute value of the time-dependent temperature profile  $\vartheta_s(t)$ , see Equation (1).

$$\left| \frac{\partial \vartheta_s}{\partial t} \right| \approx \left| \frac{\Delta \vartheta_s}{\Delta t} \right| = \left| \frac{\vartheta_s(t_1) - \vartheta_s(t_0)}{t_1 - t_0} \right| \quad (1)$$

The experimental studies to determine the cooling effect followed the schematically test bench structure shown in Figure 1a. It consisted of a heated impact plate with three thermocouples type K, a fixture for the defined nozzle placement, a controllable supply unit for a defined nozzle load with liquid CO<sub>2</sub> ( $p_{CO_2} \approx 5.7$  MPa) and compressed air, as well as a measurement data acquisition tool with thermal sensors.

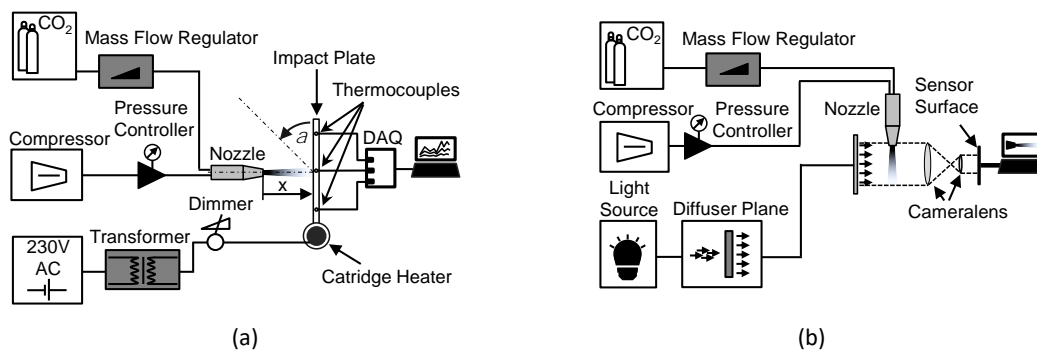


**Figure 1.** (a) Schematic test bench structure to evaluate the cooling effect. (b) Schematic test bench structure to characterize the open jet with regards to the jet intensity and jet fluctuations.

The metal plate, made from heat-treated steel AISI 4140 has a thickness of 2 mm. Three thermocouples record the time-dependent temperature change. The generated measurement signal was processed with a combined data logger consisting of a NI cDAQ-9171 & NI-9214 and recorded in a MATLAB<sup>®</sup> implemented software routine. The sample rate during the temperature measurement inside the metal plate amounts to  $f_{s,TE} = 5000$  Hz.

Prior to the test, the metal plate was preheated to an initial temperature of  $\vartheta_0 \approx 310$  °C, using a cartridge heater ( $P_{\text{cartridge}} = 400$  W). Once the plate temperature reached the target temperature, a CO<sub>2</sub>-snow jet, which is aimed at the center of the metal plate from a distance of 0.5 mm, cools the thermocouple, which is mounted beneath the metal surface. The recording time was set to  $t_m = 45$  s to ensure recording of the entire temperature curve, including the stationary minimum temperature.

The tests to evaluate the cooling effect were carried out with a cylindrical nozzle outlet. Nozzle distance and nozzle angular were varied in several stages (see Table 1), so that later recommendations could be derived concerning the integration into the modular turning tool holder. Air pressure was varied between  $p_{\text{Air}} = 0\text{--}0.8$  MPa, whereas  $p_{\text{Air}} = 0$  MPa defined the closed compressed air inlet. Furthermore, there were tests using the surrounding air pressure  $p_{\text{Air}} = p_{\infty}$ .

**Table 1.** Varied nozzle alignments and nozzle loadings using a cylindrical shaped nozzle outlet.

$\delta = 1.00$ 			Varied					Constant				
alignment	x	mm	25	30	35	-	55	$\alpha$	$\dot{m}_{CO_2}$	$p_{CO_2}$	$p_{Air}$	
		$\alpha$	$^\circ$	30	60	-	-	90	55	-	17.5	5.7
loading	$\dot{m}_{CO_2}$	kg/h	7.7	11.1	13.6	14.7	17.5	25	90	-	-	$p_\infty$
	$p_{Air}$	MPa	0.0	0.1	0.3	0.5	0.8	25	90	17.5	5.7	-

Afterwards, the influence of the nozzle shape was examined with regards to the open jet properties, the jet density and jet contour as well as the occurring open jet fluctuations, in order to achieve a good jet focus. For this purpose, a simplified shadow imaging method was used to visualize the generated CO<sub>2</sub>-snow jet with high-speed-camera recordings. This method was applicable since the densities of dry ice and air vary by a factor of 1250 and therefore, the generated open jet differentiates significantly from the surrounding area. Figure 1b shows the schematics of the used test bench, which consists of three high illuminance light sources, an optical diffuser plane to ensure an equal light scattering, a test circuit with a nozzle mount and a high-speed camera, type Imaging Solutions (High-Speed-Cam Motion Pro Y4S3). The light sources were synchronized with the high-speed camera to ensure a fixed illumination of the test bench during the tests. The camera’s exposure time was set to 3 μs. The recording frequency was set to  $f_s = 20,000$  fps with a resolution of 224 × 544 px. During each test 1000 frames were taken. The collected data was evaluated using a MATLAB<sup>®</sup> implemented software routine.

The experimental investigations for the analysis of the supply strategy of cryogenic CO<sub>2</sub>-snow cooling were carried out on a machining center, type DMG CTX beta 800 in an external longitudinal turning process. The selected technology parameters for the finishing turning of compacted graphite iron (CGI) were:  $v_c = 375$  m/min,  $f = 0.25$  mm;  $a_p = 0.5$  mm. A three-component dynamometer type Kistler 9121B was used to record the cutting force components. For the qualitative evaluation of the thermomechanical tool load, a high-speed thermographic system type FLIR<sup>®</sup> ThermoVision™ SC 6000 HS was used. The signs of wear were recorded and documented with a digital microscope type Keyence VHX-5000. The abort criteria were defined as: maximum flank wear of  $VB_{max} = 300$  μm (according to ISO 3685) or a maximum cutting length of  $L_c = 6.5$  km per workpiece.

The modular tool system (see Figure 2) is based on a PCLNL 2020 K12 turning tool holder. A reliable and user-friendly connection between the tool module and tool shaft is achieved by a specifically designed interface concept. Functional surfaces of additively manufactured components are generally reworked with conventional manufacturing processes [31] since the attainable surface quality is low by nature of the process. Surface quality measurements in the area of the inner nozzle outlet contour revealed an average roughness depth of  $R_z = 60.6$  μm or a roughness average of  $R_a = 11.6$  μm, which meets the measured surface quality scale by Stoffregen [32]. Only the threads for the connection of liquid CO<sub>2</sub> and compressed air as well as the cutting insert fixture and the functional surfaces in the area of the toggle lever clamping device were machined. The complex designed channel structures were not reworked. The integrated multi-component nozzle concept is based on pneumatic atomization, whereby the mixing of CO<sub>2</sub>-snow and compressed air takes place inside the nozzle. CGI-450 was used as the workpiece material. All three cooling supply strategies (Cryogen A: rake and flank face cooling, Cryogen B: only rake face cooling and Cryogen C: only flank face cooling) were tested by using cutting inserts out of carbide cutting grade CTCK120 produced by CERATIZIT Austria GmbH.

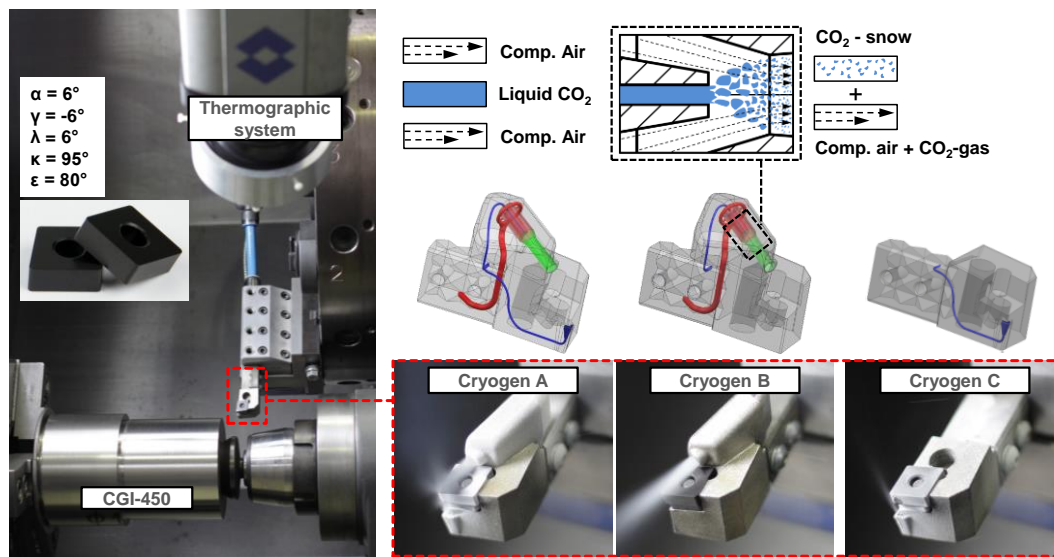


Figure 2. Experimental setup used to analyze the influence of the supply strategy with CO<sub>2</sub>-snow on the thermomechanical tool load.

### 3. Results and Discussion

#### 3.1. Examination of the Cooling Rate under Varying Nozzle Alignment and Operating Parameters

The influence of the nozzle alignment and the nozzle load were examined with a specially designed test bench (see Figure 2) to determine the cooling rate when using an additively manufactured dual nozzle with a cylindrical nozzle geometry. The experimentally determined cooling rate serves as a parameter to evaluate the cooling effect. The examined parameters are shown in Table 1. First, the influence of the nozzle alignment on the cooling rate was investigated. Figure 3 shows the influence of the distance and angular position of the nozzle on the cooling rate concerning the three different test bench temperatures  $\vartheta_s$  and with an even nozzle load. As expected, the cooling rate or the cooling effect for the used dual nozzle decreases with an increasing nozzle distance, which correlates with the observations made when using LN<sub>2</sub> [33] or CO<sub>2</sub> [34] in combination with a single component nozzle system. Thus, to ensure the highest possible cooling effect, the distance between the nozzle outlet and cutting material should be as short as possible. Furthermore, an increase of the measured cooling rate was detected when the test bench temperature  $\vartheta_s$  was enhanced. This is due to the thermodynamic relationship between heat flow and temperature difference between CO<sub>2</sub>-snow jet temperature and surface temperature. The larger the temperature difference, the higher the heat flow.

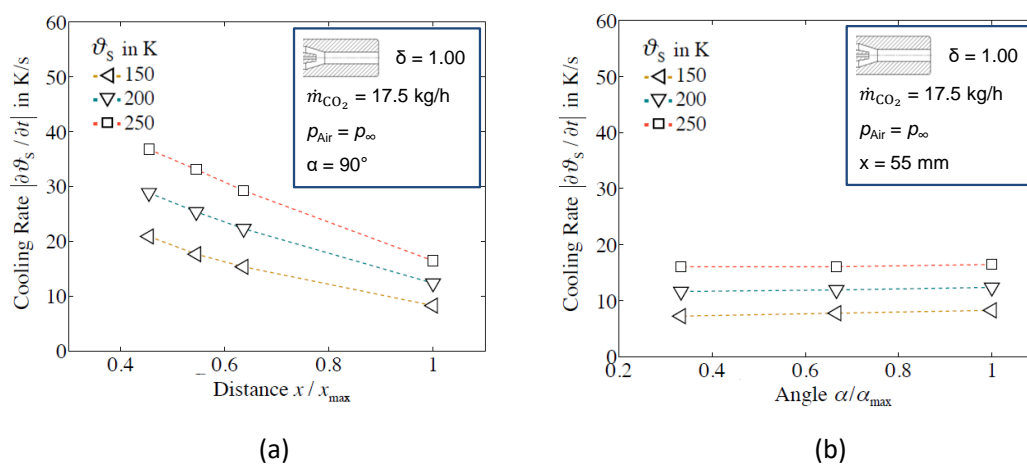


Figure 3. Influence of nozzle distance (a) and angular position of the nozzle (b) on the cooling rate.

No significant influence on the cooling rate was detected when varying the angular position of the nozzle. This observation is supported by the work of Aguilar et al. [35] on the influence of the nozzle angular between 5° and 90° on the attainable heat flow for the spray cooling with the refrigerant R-134a.

The influence of the nozzle load on the combinations of fed CO<sub>2</sub> mass flow and compressed air on the attainable cooling rate is shown in Figure 4. Both diagrams show the significant increase in cooling rate with increasing CO<sub>2</sub> mass flow as well as with an increasing amount of fed compressed air. Furthermore, this relationship is independent of the set test bench temperature  $\vartheta_s$ . An additional air-mass flow with an inlet pressure of 0.8 MPa leads to an increase of the cooling rate of 32% from 37 K/s to 49 K/s, at an even CO<sub>2</sub>-air-mass flow was of 17.5 kg/h, a constant nozzle alignment ( $\alpha = 90^\circ$ ,  $x = 25$  mm) and insert temperature ( $\vartheta = 250$  K).

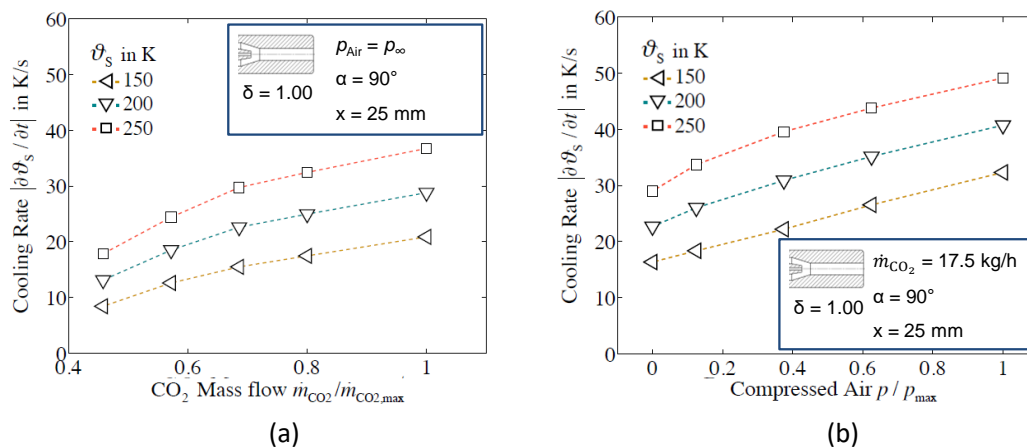


Figure 4. Influence of the supplied CO<sub>2</sub> mass flow (a) and the compressed air (b) on the cooling rate.

### 3.2. Influence of the Nozzle Opening Geometry on the Open Jet Behaviour

It is possible to increase tool life by applying a targeted cooling to the cutting process, regardless of the chosen cooling strategy [7]. To determine the suitable nozzle shape for a precise application of cryogenic multi-component CO<sub>2</sub>-snow cooling, the influence of the aperture ratio on the open jet geometry can be examined using a simplified shadow imaging process. Figure 5 shows the influence of the nozzle opening geometry of additively manufactured dual nozzles (see Figure 2) on the open jet intensity and fluctuation.

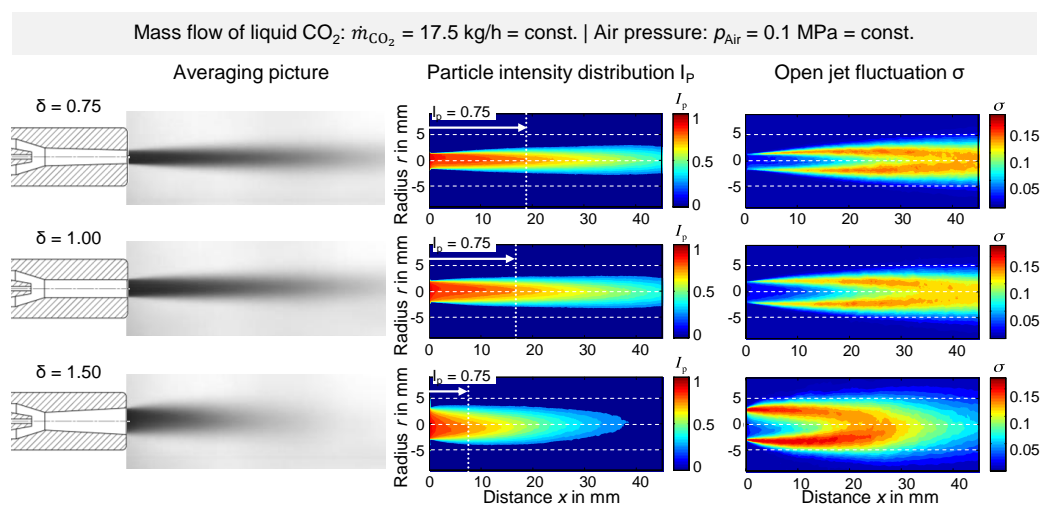


Figure 5. Influence of the nozzle aperture ratio on open jet intensity and open jet fluctuation.

The local grey tone distribution is an important indicator for the local CO<sub>2</sub>-snow-particle intensity. For the interpretation of the measured high-speed recordings the following applies: the darker the grey tone of a pixel, the higher the particle intensity (see Figure 5). To determine the particle intensity for the entire recording time, first the average grey tone distribution of each pixel is determined for each recorded frame. Then the averaged particle intensity for the measured number of frames is determined. Another statistically significant parameter for the evaluation of the open jet fluctuation, when varying the nozzle geometry, is the calculation of the standard derivation for the temporal grey tone distribution over a number of  $n = 1000$  images, see Equation (2).

$$\sigma_{x,y} = \sqrt{\frac{1}{n-1} \sum_{i=1}^n (P_{x,y,i} - \bar{P}_{x,y})^2} \quad (2)$$

A convergent shaped nozzle geometry ( $\delta = 0.75$ ) leads to a focused jet and an increase in the axial jet length when using cryogenic multi-component cooling with CO<sub>2</sub>-snow. A divergent nozzle geometry ( $\delta = 1.50$ ), on the other hand, leads to an expansion and shortening of the resulting jet. Considering the influence of the nozzle geometry on the jet fluctuation  $\sigma$ , the convergent as well as cylindrical shaped nozzle outlet show a pronounced stable jet core with an axial length of approximately 18 mm. The divergent nozzle geometry, on the other hand, shows a barely stable core area. The stable jet core has an axial length of less than 10 mm. Consequently, the intensity fluctuations for divergent nozzle geometries are higher than the intensity fluctuations of cylindrical or convergent geometries. The explanation for these increased fluctuations is the divergent geometries of the nozzle itself. The bigger the nozzle's aperture ratio, the bigger the opening angle. The danger of a flow separation in the divergent part of the nozzle, which acts as a diffusor when the aperture ratio is bigger than 1, occurs with an increasing opening angle [36]. Flow separation inside the nozzle's wall, is likely to lead to an unstable distribution of the particle intensity. The nozzle selection in this work is supported by the results from Pereira et al. [15], which also used a convergent shaped nozzle geometry due to an increased jet focus by 1.7 in comparison with divergent nozzle shapes.

### 3.3. Influence of the Supply Strategy on the Thermomechanical Tool Load

First, the thermomechanical tool load for sharp cutting inserts ( $VB_{\max} \leq 50 \mu\text{m}$ ) was determined in comparison to dry machining. Figure 6 shows the result of the acting thermomechanical load with varying cooling strategies. Compared to dry machining, the application of cryogenic CO<sub>2</sub>-snow leads to an increase in all cutting force components. A holistic view of temperature and cutting force measurement with sharp cutting inserts shows a fundamental shift in the thermomechanical tool load in the sense of increased mechanical load and reduced thermal load.

The reason for this is the excellent cooling effect of CO<sub>2</sub>-snow. With a lower thermal load in the area of the cutting zone, the mechanical material strength increases and leads to an increase in machining forces, compared to dry machining. This conclusion is supported by previous work carried out by both Hong et al. [4] concerning the turning of TiAl6V4 under cryogenic cooling with liquid nitrogen, and by Pfeiffer [2] concerning the turning of CGI-450 under CO<sub>2</sub>-snow cooling. In contrast, Kumar et al. [37] and Jerold et al. [38] observed a decrease in cutting force when turning steel materials under cryogenic cooling with liquid nitrogen or CO<sub>2</sub>-snow, compared to dry machining. Machai et al. [39] on the other hand could not detect any increase in cutting force when turning Ti-10V-2Fe-3Al under rake face cooling with CO<sub>2</sub>-snow. This shows that the relationship between cryogenic cooling strategies and thermomechanical tool load is not fully clarified and that further investigations are required.

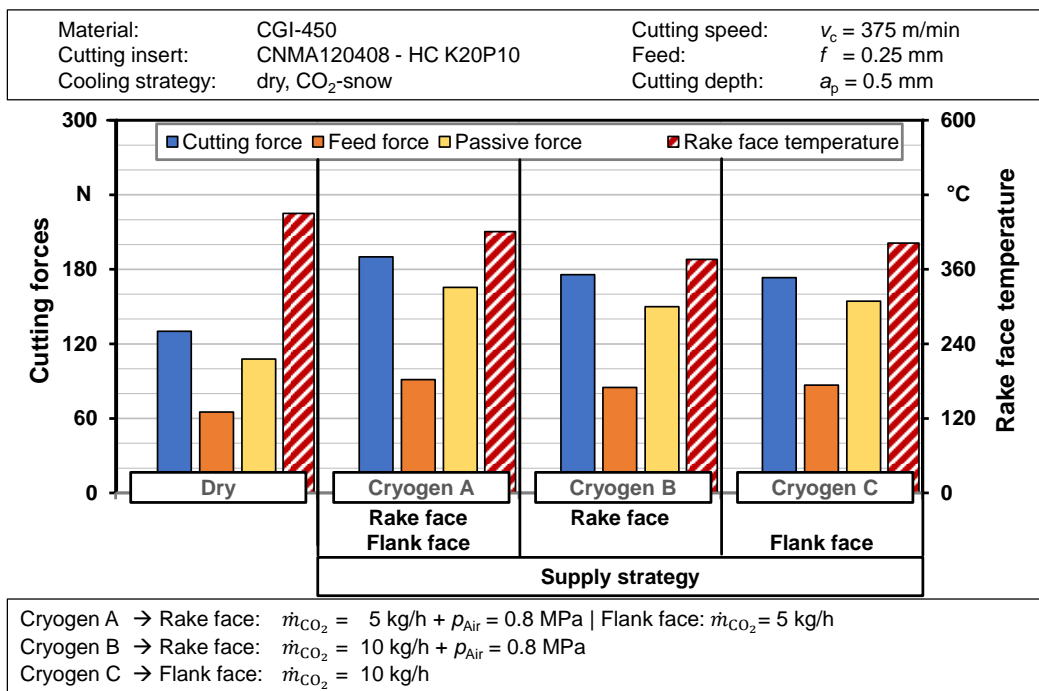


**Figure 6.** Thermomechanical tool load using sharp cutting inserts with different cooling strategies compared to dry machining.

Figure 7 depicts the signs of wear after reaching the previously defined abort criteria with reference to dry machining. The wear mechanisms detected during dry machining are a combination of abrasion and adhesion whereas under cryogenic cooling conditions, abrasion is primarily observed. Due to the lack of rake face cooling in the “Cryogen C” cooling strategy, both a pronounced thermal zone of influence and a pronounced crater wear behavior are detected. With increased rake face cooling, the crater wear is reduced and reaches its minimum within the scope of this test series under cooling strategy “Cryogen B”. The analysis of the supply strategy shows that a focused cooling of the rake face is essential to effectively minimize the thermal load of the cutting insert, and thus considerably reduces crater wear.

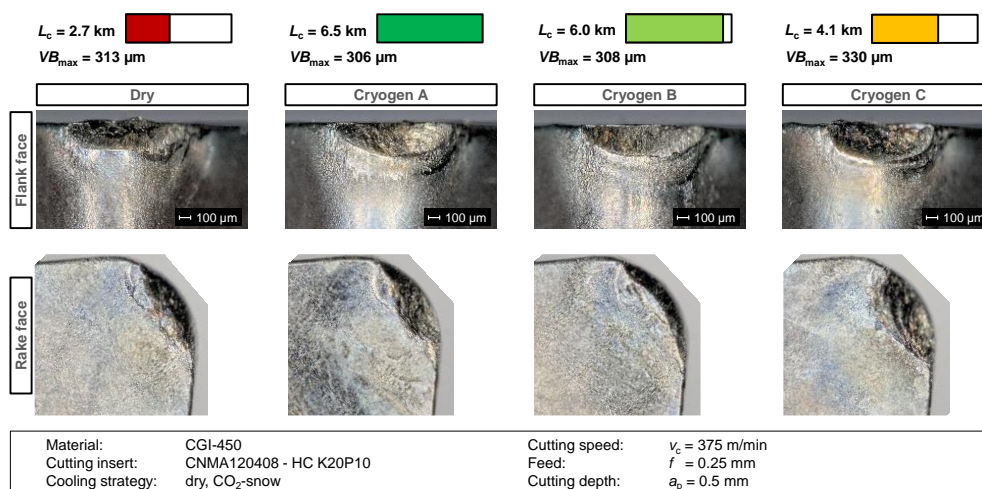


**Figure 7.** Signs of wear after reaching the abort criteria when using CO<sub>2</sub>-snow compared to dry machining.

#### 4. Conclusions

This work presented an additively manufactured modular turning tool holder with an integrated dual nozzle for the targeted and process-reliable application of cryogenic CO<sub>2</sub>-snow jet cooling. A focused open jet behavior could be achieved using convergent shaped nozzle geometry. The following insights and recommendations for action can be derived:

- The nozzle distance affects the ability to achieve cutting edge cooling more strongly than the angular alignment of the nozzle.
- The cooling rate for cryogenic CO<sub>2</sub>-snow jet cooling is increased by 32% with an additional air-mass flow.
- The long-term behavior regarding process-reliability (protecting the nozzle against ice formation) was improved significantly using CO<sub>2</sub>-snow jets with dual nozzles compared to a single-component nozzle.
- Efficient rake face cooling is essential for the reduction of thermal tool loads and has a significant effect on the crater wear behavior.
- The wear development on the flank face can be further reduced by targeted flank face cooling.
- Compared to dry machining, the tool life  $L_c$  could be increased by a factor of 2.4 with combined rake face and flank face cooling using CO<sub>2</sub>-snow.

In this study, it was shown that the chosen supply strategy of using cryogenic cooling with CO<sub>2</sub>-snow has a significant influence on the thermomechanical tool load, and is therefore a key factor in the operating behavior of high-performance cutting materials.

**Author Contributions:** Supervision, E.A.; Funding Acquisition, E.A.; Project Administration, T.H.; Conceptualization, T.H., C.B. and E.A.; Methodology, T.H. and C.B.; Validation, T.H., C.B. and E.A.; Investigation, T.H. and C.B.; Visualization, T.H. and C.B.; Writing-Original Draft Preparation, T.H. and C.B.; Writing-Review & Editing, T.H.

**Funding:** This research was funded by German Research Foundation (DFG), grant number AB 133/99-1.

**Acknowledgments:** The authors extend their sincerest gratitude to the German Research Foundation (DFG) for the generous support of the work described in this paper.

**Conflicts of Interest:** The authors declare no conflict of interest.

#### References

1. Bordin, A.; Sartori, S.; Bruschi, S.; Ghiotti, A. Experimental investigation on the feasibility of dry and cryogenic machining as sustainable strategies when turning Ti6Al4V produced by Additive Manufacturing. *J. Clean. Prod.* **2017**, *142*, 4142–4151. [[CrossRef](#)]
2. Pfeiffer, P. Technologische Prozessauslegung für die Zerspanung von Gusseisen mit Vermiculargrafit unter kontinuierlichen Schnittbedingungen. Ph.D. Thesis, TU Darmstadt, Darmstadt, Germany, 2014.
3. Biermann, D.; Abrahams, H.; Metzger, M. Experimental investigation of tool wear and chip formation in cryogenic machining of titanium alloys. *Adv. Manuf.* **2015**, *3*, 292–299. [[CrossRef](#)]
4. Hong, S.Y.; Ding, Y.; Jeong, W. Friction and cutting forces in cryogenic machining of Ti-6Al-4V. *Int. J. Mach. Tools Manuf.* **2001**, *41*, 2271–2285. [[CrossRef](#)]
5. Weinert, K.; Hesterberg, S.; Wittkop, S. Den Span eiskalt erwischt. *Werkstatt und Betr. Wb* **2003**, *136*, 74–76.
6. Ueda, T.; Hosokawa, A.; Yamada, K. Effect of Oil Mist on Tool Temperature in Cutting. *J. Manuf. Sci. Eng.* **2006**, *128*, 130–135. [[CrossRef](#)]
7. Bermingham, M.J.; Palanisamy, S.; Kent, D.; Dargusch, M.S. A comparison of cryogenic and high pressure emulsion cooling technologies on tool life and chip morphology in Ti-6Al-4V cutting. *J. Mater. Process. Technol.* **2012**, *212*, 752–765. [[CrossRef](#)]
8. Abele, E.; Schramm, B. Using PCD for machining CGI with a CO<sub>2</sub> coolant system. *Prod. Eng.* **2008**, *2*, 165–169. [[CrossRef](#)]
9. Kaynak, Y.; Gharibi, A. Progressive Tool Wear in Cryogenic Machining: The Effect of Liquid Nitrogen and Carbon Dioxide. *J. Manuf. Mater. Process.* **2018**, *2*, 31. [[CrossRef](#)]

10. Blau, P.; Busch, K.; Dix, M.; Hochmuth, C.; Stoll, A.; Wertheim, R. Flushing Strategies for High Performance, Efficient and Environmentally Friendly Cutting. *Procedia CIRP* **2015**, *26*, 361–366. [[CrossRef](#)]
11. Jawahir, I.S.; Attia, H.; Biermann, D.; Duflou, J.; Klocke, F.; Meyer, D.; Newman, S.T.; Pusavec, F.; Putz, M.; Rech, J.; et al. Cryogenic manufacturing processes. *CIRP Ann.* **2016**, *65*, 713–736. [[CrossRef](#)]
12. Gross, D.; Heinz, A.; Ebner, M.; Hanenkamp, N. Assessment of Process Improvement Potential of Carbon Dioxide as a Cryogenic for Machining Operations. *Appl. Mech. Mater.* **2017**, *856*, 151–158. [[CrossRef](#)]
13. Tapoglou, N.; Lopez, M.I.A.; Cook, I.; Taylor, C.M. Investigation of the influence of CO<sub>2</sub> cryogenic coolant application on tool wear. *Procedia CIRP* **2017**, *63*, 745–749. [[CrossRef](#)]
14. Lin, T.-C.; Hong, C.Y.; Shen, Y.L.; Wang, M.R. Effects of Bypass Flow on CO<sub>2</sub> Snow Formation for Cryogenic Application. *J. Aeronaut. Astronaut. Aviat.* **2012**, *44*, 193–200.
15. Pereira, O.; Rodriguez, A.; Barreiro, J.; Fernández-Abia, A.I.; López de Lacalle, L.N. Nozzle Design for Combined Use of MQL and Cryogenic Gas in Machining. *Int. J. Precis. Eng. Manuf. Green Technol.* **2017**, *4*, 87–95. [[CrossRef](#)]
16. Montandon, J. Energiesparen mit 3D-gedruckten KSS-Düsen. In Proceedings of the Schweizer Schleif-Symposium, Zurich, Switzerland, 19–20 January 2016.
17. Wegener, K.; Bleicher, F.; Krajnik, P.; Hoffmeister, H.; Brecher, C. Recent developments in grinding machines. *CIRP Ann.* **2017**, *66*, 779–802. [[CrossRef](#)]
18. Bourell, D.; Kruth, J.P.; Leu, M.; Levy, G.N.; Rosen, D.; Beese, A.M.; Clare, A. Materials for additive manufacturing. *CIRP Ann.* **2017**, *66*, 659–681. [[CrossRef](#)]
19. Schmidt, M.; Merklein, M.; Bourell, D.; Dimitrov, D.; Hausotte, T.; Wegener, K.; Overmeyer, L.; Vollertsen, F.; Levy, G.N. Laser based additive manufacturing in industry and academia. *CIRP Ann.* **2017**, *66*, 561–583. [[CrossRef](#)]
20. Kress, D. Mittels eines Lasersinterverfahrens hergestellter Bohrer. Patent WO2015/166065 A1, 5 November 2015.
21. Ach, E.; Gey, C. Zerspanungswerkzeug sowie Verfahren zum Herstellen eines Zerspanungswerkzeugs. Patent DE102014207507 A1, 22 October 2015.
22. Donisi, S.; Graf, G. Scheibenfräser und Herstellverfahren. Patent DE102014012481 A1, 3 March 2016.
23. Kappmeyer, G. Verfahren zur Herstellung eines Zerspanwerkzeugs. Patent DE102006026967 A1, 13 December 2007.
24. Biermann, D.; Meier, H.; Haberland, C.; Abrahams, H.; Metzger, M.; Steiner, M. Einsatz additiv gefertigter Werkzeughalter—Optimierungspotentiale bei der Drehbearbeitung von Titan durch strahlgeschmolzene Werkzeugaufnahmen. *wt Werkstattstech. online* **2013**, *103*, 481–484.
25. Seidel, C.; Kamps, T.; Riss, F.K.E. Bio TRIZ—Process know-how, design methodologies and software tools for enhanced additive manufacturing. In Proceedings of the Symposium of Additive Manufacturing and Innovative Technologies (Add+it), Linz, Austria, 10–11 September 2015.
26. Uhlmann, E.; Peukert, B.; Thom, S.; Prasol, L.; Fürstmann, P.; Sammler, F.; Richarz, S. Solutions for Sustainable Machining. *J. Manuf. Sci. Eng.* **2017**, *139*, 051009-1–051009-7. [[CrossRef](#)]
27. Denkena, B.; Grove, T.; Kuhlemann, P. Geschlossenes Kühlsystem vermeidet Osteonekrose. *Werkstatt und Betr. WB* **2016**, *149*, 42–45.
28. Ward, H.; Burger, M.; Chang, Y.; Fürstmann, P.; Neugebauer, S.; Radebach, A.; Sproesser, G.; Pittnerac, A.; Rethmeier, M.; Uhlmann, E.; et al. Assessing carbon dioxide emission reduction potentials of improved manufacturing processes using multiregional input output frameworks. *J. Clean. Prod.* **2017**, *163*, 154–165. [[CrossRef](#)]
29. Abele, E.; Heep, T. Feinbearbeitung von Vermicularguss bei Einsatz eines additiv gefertigten Drehhalters für die Prozesskühlung mit CO<sub>2</sub>-Schnee. In *Spanende Fertigung—Prozesse, Innovationen, Werkstoffe*; Biermann, D., Ed.; Vulkan-Verlag GmbH: Essen, Germany, 2017; Volume 7, pp. 48–56. ISBN 978-3-8027-2989-8.
30. Heep, T.; Abele, E. Additively manufactured turning tool solution for the application of cryogenic CO<sub>2</sub>-cooling. In Proceedings of the 14th Powertrain Manufacturing Conference, Darmstadt, Germany, 21–22 November 2017.
31. Gibson, I.; Rosen, D.W.; Stucker, B. *Additive Manufacturing Technologies*; Springer Science + Business Media: New York, NY, USA, 2010; ISBN 978-1-4419-1119-3.
32. Stoffregen, H.A. Strukturintegration piezoelektrischer Vielschichtaktoren mittels selektiven Laserschmelzens. Ph.D. Thesis, TU Darmstadt, Darmstadt, Germany, 2015.

33. Kraemer, A. Gestaltungsmodell der kryogenen Prozesskühlung in der Zerspanung. Ph.D. Thesis, RWTH Aachen, Aachen, Germany, 2015.
34. Liu, Y. Analysis of Production Process of Fine Dry Ice Particles and Application for Surface Cleaning. Ph.D. Thesis, Kyoto University, Kyoto, Japan, 2012.
35. Aguilar, G.; Vu, H.; Nelson, J.S. Influence of angle between the nozzle and skin surface on the heat flux and overall heat extraction during cryogen spray cooling. *Phys. Med. Biol.* **2004**, *49*, N147–N153. [[CrossRef](#)] [[PubMed](#)]
36. Spurk, J.H.; Aksel, N. *Fluid Mechanics*, 2nd ed.; Springer: Berlin/Heidelberg, Germany, 2008; ISBN 978-3-540-73536-6.
37. Kumar, K.K.; Choudhury, S.K. Investigation of tool wear and cutting force in cryogenic machining using design of experiments. *J. Mater. Process. Technol.* **2008**, *203*, 95–101. [[CrossRef](#)]
38. Jerold, B.D.; Kumar, M.P. Experimental comparison of carbon-dioxide and liquid nitrogen cryogenic coolants in turning of AISI 1045 steel. *Cryogenics* **2012**, *52*, 569–574. [[CrossRef](#)]
39. Machai, C.; Biermann, D. Machining of beta-titanium-alloy Ti-10V-2Fe-3Al under cryogenic conditions: Cooling with carbon dioxide snow. *J. Mater. Process. Technol.* **2011**, *211*, 1175–1183. [[CrossRef](#)]



© 2019 by the authors. Licensee MDPI, Basel, Switzerland. This article is an open access article distributed under the terms and conditions of the Creative Commons Attribution (CC BY) license (<http://creativecommons.org/licenses/by/4.0/>).